ISSN 1949-8470 (online)

World Journal of *Radiology*

World J Radiol 2017 December 28; 9(12): 416-458

Published by Baishideng Publishing Group Inc

WJR World Journal of Radiology

Contents

Monthly Volume 9 Number 12 December 28, 2017

REVIEW

MINIREVIEWS

CASE REPORT

World Journal of Radiology
Volume 9 Number 12 December 28, 2017

Contents

NAME OF JOURNAL
World Journal of Radiology

ISSN
ISSN 1949-8470 (online)

LAUNCH DATE
January 31, 2009

FREQUENCY
Monthly

EDITORIAL OFFICE
Xiu-Xia Song, Director
World Journal of Radiology
Baishideng Publishing Group Inc
7901 Stoneridge Drive, Suite 501, Pleasanton, CA 94588, USA
Telephone: +1-925-2238242
Fax: +1-925-2238243
E-mail: editorialoffice@wjgnet.com
Help Desk: http://www.f6publishing.com/helpdesk
http://www.wjgnet.com

PUBLISHER
Baishideng Publishing Group Inc
7901 Stoneridge Drive, Suite 501,
Pleasanton, CA 94588, USA
Telephone: +1-925-2238242
Fax: +1-925-2238243
E-mail: bpgoffice@wjgnet.com
Help Desk: http://www.f6publishing.com/helpdesk
http://www.wjgnet.com

PUBLICATION DATE
December 28, 2017

INSTRUCTIONS TO AUTHORS
http://www.wjgnet.com/bpg/gerinfo/204

ONLINE SUBMISSION
http://www.f6publishing.com

World Journal of Radiology

Submit a Manuscript: http://www.f6publishing.com

World J Radiol 2017 December 28; 9(12): 416-425

DOI: 10.4329/wjr.v9.i12.416

ISSN 1949-8470 (online)

REVIEW

Dynamic contrast-enhanced magnetic resonance imaging of prostate cancer: A review of current methods and applications

Yousef Mazaheri, Oguz Akin, Hedvig Hricak

Yousef Mazaheri, Department of Medical Physics and Radiology, Memorial Sloan Kettering Cancer Center, New York, NY 10065, United States

Oguz Akin, Hedvig Hricak, Department of Radiology, Memorial Sloan Kettering Cancer Center, New York, NY 10065, United States

ORCID number: Yousef Mazaheri (0000-0002-8493-1608); Oguz Akin (0000-0002-2041-6199); Hedvig Hricak (0000-0003-2240-9694).

Author contributions: All authors are the guarantors of integrity of entire study; Mazaheri Y designed the study; Mazaheri Y and Akin O performed data analysis/interpretation; Mazaheri Y and Akin O performed the literature research; all authors contributed to manuscript drafting or manuscript revision for important intellectual content; all authors gave manuscript final version approval and manuscript editing; all authors take responsibility for the integrity of the data and the accuracy of the data analysis.

Conflict-of-interest statement: This manuscript is not published anywhere else; all authors conform that there is no conflict of interests (including none for related to commercial, personal, political, intellectual, or religious interests).

Manuscript source: Unsolicited manuscript

Correspondence to: Yousef Mazaheri, PhD, Department of Medical Physics and Radiology, Memorial Sloan Kettering Cancer Center, 1275 York Avenue, New York, NY 10065, United States. mazahery@mskcc.org
Telephone: +1-646-8884520
Fax: +1-646-8885139

Received: May 17, 2017
Peer-review started: May 19, 2017
First decision: July 3, 2017
Revised: August 3, 2017
Accepted: October 17, 2017
Article in press: October 17, 2017
Published online: December 28, 2017

Abstract

In many areas of oncology, dynamic contrast-enhanced magnetic resonance imaging (DCE-MRI) has proven to be a clinically useful, non-invasive functional imaging technique to quantify tumor vasculature and tumor perfusion characteristics. Tumor angiogenesis is an essential process for tumor growth, proliferation, and metastasis. Malignant lesions demonstrate rapid extravasation of contrast from the intravascular space to the capillary bed due to leaky capillaries associated with tumor neovascularity. DCE-MRI has the potential to provide information regarding blood flow, areas of hypoperfusion, and variations in endothelial permeability and microvessel density to aid treatment selection, enable frequent monitoring during treatment and assess response to targeted therapy following treatment. This review will discuss the current status of DCE-MRI in cancer imaging, with a focus on its use in imaging prostate malignancies as well as weaknesses that limit its widespread clinical use. The latest techniques for quantification of DCE-MRI parameters will be reviewed and compared.

Key words: Prostate cancer; Prostate magnetic resonance imaging; Tumor angiogenesis; Dynamic contrast-enhanced magnetic resonance imaging; K_{ep} = rate constant between extracellular extravascular space and plasma space; K^{trans} = volume transfer constant

Core tip: Dynamic contrast-enhanced magnetic resonance imaging (DCE-MRI) of prostate cancer can characterize tissue vascularity with important clinical application including aid in the detection, localization and staging, assessment of tumor aggressiveness, and assessment of treatment response. The current lack of standardized acquisition and analysis methods should be addressed to encourage more wide spread use of DCE-MRI in prostate cancer imaging.

Mazaheri Y, Akin O, Hricak H. Dynamic contrast-enhanced magnetic resonance imaging of prostate cancer: A review of current methods and applications. *World J Radiol* 2017; 9(12): 416-425 Available from: URL: http://www.wjgnet.com/1949-8470/full/v9/i12/416.htm DOI: http://dx.doi.org/10.4329/wjr.v9.i12.416

INTRODUCTION

This review describes dynamic contrast-enhanced magnetic resonance imaging (DCE-MRI) techniques for aiding prostate cancer management. First, we review methodologies for the acquisition and analysis of DCE-MRI data, including a commonly used model for the quantification of DCE-MRI data sets. Second, we discuss several current and potential future clinical applications of DCE-MRI and pharmacokinetic parametric maps in prostate cancer imaging. These include: (1) Primary tumor detection, localization, and staging; (2) risk assessment; (3) treatment planning; (4) treatment response assessment; and (5) detection of residual or locally recurrent cancer after treatment. Finally, we present an overview of the challenges of DCE-MRI in the management of prostate cancer and future directions.

BASIC CONCEPTS

To characterize tumor vasculature, a number of paramagnetic agents have been approved for routine clinical use. The most commonly-used contrast agents are gadolinium (Gd) chelates of low molecular weight. The mechanism of most T_1 methods involves characterization of the influxes and out-fluxes of the contrast agent and of the extracellular extravascular volume fraction within the tumor vasculature. In conventional contrast-enhanced imaging, data are acquired before contrast administration and again one or two times after contrast administration. An intravenous line may be set up during or prior to the exam to allow the injection of gadolinium contrast [gadolinium-diethylenetriamine pentaacetic acid (Gd-DTPA)] during a magnetic resonance (MR) acquisition. For some patients, Gd-DTPA may be injected into the arm by a nurse, just as is done for many routine clinical MRI exams. Gd-DTPA is administered into the right antecubital vein.

DCE-MRI is the acquisition of sequential images during the passage of a contrast agent within a tissue of interest. DCE-MRI data are acquired rapidly during imaging following IV injection of the contrast agent and allow modeling of the passage of the contrast agent. Numerous pharmacokinetic models have been proposed for quantitative analysis of the observed signal intensity changes following contrast agent administration and for estimating pharmacokinetic parameters[1,2]. For a comprehensive review of DCE-MRI tracer kinetic models see[3] as well as a recent article by Sourbron and Buckley[4].

IMAGING STRATEGIES: RAPID DYNAMIC CONTRAST-ENHANCED IMAGING

In "dynamic" contrast-enhanced MR imaging, 3D T_1-weighted fast spoiled gradient-echo MRI sequences are obtained every 5-10 s before, during, and several minutes after administration of contrast in a sequential or "dynamic" fashion for a period of up to 10 min. Acquisition times of greater than 15 s are generally not used due to difficulty detecting early enhancement and capillary transit time of < 5 s. Contrast agents create shorter relaxation times, resulting in a brightening of T_1 signal on images. Contrast signal depends on both extravasation of contrast as well as velocity of blood flow to the target area[5,6]. There is no consensus on the best method for acquiring DCE-MRI data.

QUANTIFICATION OF DCE-MRI DATA

The assessment of signal enhancement after contrast injection can be performed through a semi-quantitative analysis of signal intensity changes over time. In this approach parameters, including curve shape, maximum signal intensity, wash-in (or upslope) and washout rates, as well as the initial area under the signal intensity curve or contrast medium concentration (IAUGC) curve, are estimated. Alternatively, it is possible to use a quantitative approach, which is based on pharmacokinetic modeling of the contrast agent. Numerous pharmacokinetic models have been proposed for quantitative analysis of signal intensity changes and for estimating pharmacokinetic parameters[1,2].

Semi-quantitative/model-free method

Data modeling impacts the accuracy of parameters derived from DCE-MR images, which depends on both temporal sampling and signal intensity from the injected contrast agent. As an alternative to data modeling, data can be compared in a semi-quantitative method by using pixel-by-pixel analysis[4,6]. From the corresponding signal intensity–time curves, enhancement kinetic parameters, semi-quantitative parameters are estimated. The typical parameters estimated for the semi-quantitative or non-model-based analysis include peak enhancement (PE), time-to-peak (TTP), wash-in, washout, and IAUGC. PE refers to the maximum signal intensity value between contrast arrivals, normalized by subtraction of the baseline

signal intensity. The quantity TTP is the corresponding time when the peak-enhancement is observed. The enhancement-slope and washout-slope allow for the quantitative evaluation of the wash-in and wash-out of the contrast agent and refer to the steepness of the curve during wash-in and wash-out (until the end of the acquisition), respectively. Semi-quantitative parameters are readily calculated with post-processing software available from the manufacturer of the MR unit and do not require measurement of arterial input function or tissue T_1 relaxation. One notable disadvantage of semi-quantitative parameters is that they are estimated directly from the signal intensity measurements (or concentration if in addition T_1 maps are generated) without a physiological or empirical model. Another disadvantage is that these parameters are dependent on experimental factors such as hardware, sequence parameters, and contrast dose, which limit their comparability across different sites or different acquisitions under different experimental conditions.

The semi-quantitative analyses provide parameters of area under the curve, time to peak, maximum enhancement, and slope of regions of interest. Advantages of these analytical parameters are their ease of acquisition, good visual image quality, and the fact that they do not require additional information such as tissue T_1 or measurement of the arterial input function. However, variability in dosing, bolus time, sequence parameters, tissue characteristics or other factors could affect reproducibility, presenting problems when utilizing these descriptive parameters. Models have been utilized to quantify and standardize parameters of contrast agents.

Quantitative analysis of DCE-MRI

A number of methods have been presented in the literature for the acquisition and analysis of DCE-MRI data sets. In this section we will review the basic principles of DCE-MRI analysis and introduce a few widely used analysis methods.

Relationship between MR signal and contrast agent concentration

In contrast-enhanced MRI, the relationship between signal and contrast agent concentration is not linear. To estimate contrast agent concentration, required for quantification of DCE-MRI parameters, the relationship between T_1, signal intensity, and contrast agent concentration is applied. The signal intensity for a spoiled gradient echo in steady-state is given by: $S(\alpha) = M_0 [(1-E_1) \sin(\alpha)]/[1-E_1 \cos(\alpha)] \times e^{(-TE/T2^*)}$ [1].

Where $E1 = e^{-(TE/T1)}$, α is the flip angle, M_0 is the proton density, TR is the repetition time, TE is the echo time, and T_2^* is the effective transversal relaxation time. The change in relaxation rate per unit of contrast agent concentration is given by[7], assuming that the tracer concentration is to be linearly proportional to the change in the relaxation rate under the assumption of a fast exchange limit: $C(t) = (1/R_1)\{[1/T_1(t)] - [1/T_1(0)]\}$ [2].

Where $T_1(t)$ and $T_1(t)$ are the relaxation times with contrast agent at time *t*, and pre-enhancement, R_1 is the relaxivity in $(mM \cdot s)^{-1}$ taken to equal 4.5 mmol/s at 1.5-Tesla field strength, and C (t) is the concentration of the contrast agent.

Tofts model

Following the convention proposed by Tofts *et al*[8], a simple one-compartmental model of the tumor is used to predict the flow of the contrast agent into the EES as a function of time (Figure 1): $[d C_t(t)]/dt = K^{trans} \times \{C_p(t) - [C_t(t)/v_e]\}$ [8].

Where $C_p(t)$ is the tracer concentration in blood plasma $C_p = C_b/(1\text{-Hct})$, and the hematocrit (Hct) in tumors is typically assumed to equal 0.25[9]. K^{trans} (min) is the volume transfer constant between the blood plasma and the EES; K_{ep} (min) is the rate constant between the EES and the blood plasma and is given by: $K_{ep} = (K^{trans}/v_e)$ where v_e is the fractional volume of the EES. Intuitively, K^{trans} describes the diffusive transport of the contrast agent across the capillary endothelium. The solution to Eq.[8], with the assumption that the contribution to the concentration of the contrast agent due to plasma is negligible, is given by the following (referred to as the original Tofts model): $C_p(t) = K^{trans} \int_0^t C_p(u) \times \exp\{-[K^{trans}(t-u)]/v_e\} du$ [9].

Extended Tofts model (ETM)

In the case of tumors, the above-mentioned assumption is not valid, and thus the two-compartment extension of the Tofts model is required, where the tissue concentration is the sum of the contribution due to the plasma volume, v_p, as well as the fractional volume of the EES, v_e: $C_t(t) = v_p C_p(t) + v_e C_e(t)$ [10].

The extended Tofts model corresponds to two compartments with the assumption that the concentration of the contrast agent is derived from the EES and plasma, given by: $C_t(t) = K^{trans} \int_0^t C_p(u) \times \exp\{-[K^{trans}(t-u)]/v_e\} du + v_p C_p(t)$ [11].

Additional considerations in quantitative DCE-MRI

A number of factors need to be taken into account in the estimation of parameters from DCE-MRI.

Choice of arterial input function

Measurement of the patient-specific arterial input function (AIF) or plasma concentration requires localization of a large vessel that delivers blood to the organ of interest. Alternatively a bi-exponential AIF, $C_p(t)$, can be generated assuming a bi-exponent model given by[10] (Figure 2): $C_p(t) = D[a_1 \exp(-m_1 t) + a_2 \exp(-m_2 t)]$ [10].

Where *D* is the dose of the contrast agent (mmol/kg of body weight). This is referred to as a model-based AIF. The first term in this expression corresponds to the equilibration of contrast agent between blood and extracellular space (fast), while the second term

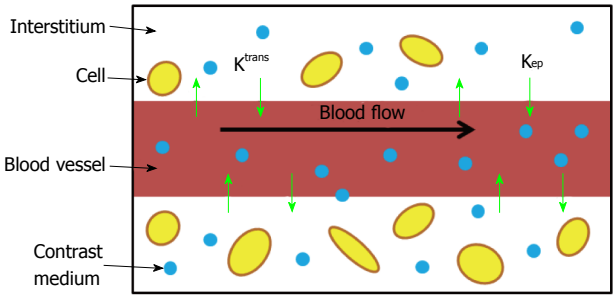

Figure 1 Schematic diagram of the Tofts kinetic model with the commonly used estimated parameters K^{trans} and k_{ep}.

corresponds to the removal of contrast agent from the plasma by the kidneys (slow). Substituting Eq.[10] into Eq.[8] and solving for $C_t(t)$ in the tumor tissue we obtain: $C_p(t) = D \times K^{trans} \Sigma^{2}_{i=1} \{[a_1 \exp(-m_i t) + a_2 \exp(-k_{ep} t)]/k_{ep}-m_i\}$ [11].

An alternative to calculating the bi-exponential AIF is to derive the AIF in a select population and extend it to future studies. This is referred to as a population average AIF. One study compared prostate DCE-MRI parameters obtained at 3 Tesla before biopsy using three AIF estimates: Patient-specific or individual AIF, population average AIF, and model-based AIF[11]. The study found patient-specific and population average AIFs had the highest sensitivity in predicting the biopsy results in prostate cancer, while the model-based bi-exponential AIF had the highest specificity. The areas under the ROC curves were not significantly different between any of the AIFs. In another study[12], investigators compared the effects of using population based AIF or semi-automated or fully automated image-based patient-specific AIF to calculate DCE-MRI parameters in the prostate; they found that K^{trans} estimates were more sensitive to the choice between population *vs* patient-specific AIF as compared to k_{ep}.

T_1 mapping

An estimate of the voxel contrast concentration in DCE-MRI requires T_1 estimation in order to convert signal intensity to T_1 values. T_1 relaxation times can be estimated from T_1 maps acquired prior to the injection of contrast. Typically, before contrast agent administration, a series of spoiled gradient echo volumes at different flip angles are acquired[13]. The steady-state signal is given by Eq.[1], which can be rearranged to yield: $S(\alpha)/\sin(\alpha) = E_1 [S(\alpha)/\tan(\alpha)] + M_0 \times (1-E_1) \times e^{(-TE/T^*2)}$ [12].

With a series of acquisitions at different flip angles, a linear fit of $S(\alpha)/\sin(\alpha)$ *vs* $S(\alpha)/\tan(\alpha)$ will allow estimation of T_1 from a linear fit $T_1 = -TR/\ln(m)$, where m is the slope between measurement points. At least two flip angles are required to estimate T_1 maps.

DCE-MRI of prostate

Studies on the use of dynamic or conventional contrast-enhanced MRI for prostate cancer have focused on localization and staging, assessment of prostate cancer aggressiveness, and assessment of treatment response (Figure 3). These studies suggest the many ways that contrast-enhanced MRI could be used to augment the value of a prostate MRI exam.

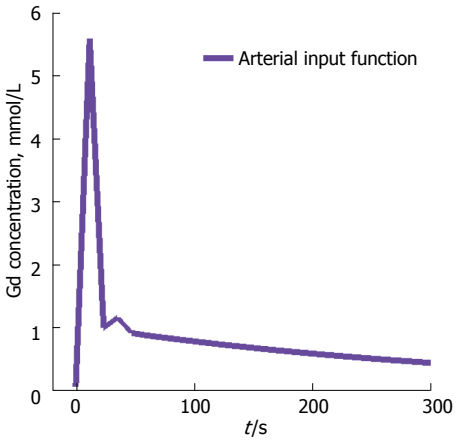

Figure 2 Model-based arterial input function. Shown is the model-based arterial input function, based on the Parker function.

Localization and staging

Numerous studies have investigated the accuracy of DCE-MRI in localization and staging of prostate cancer using DCE-MRI (Figures 4 and 5). In a study performed at 1.5 Tesla, the accuracy of DCE-MRI in tumor localization was found to be significantly higher than that of T2-weighted imaging (as well as significantly higher than that of quantitative spectroscopic imaging)[14]. The same group reported that accuracy in prostate cancer localization (again at 1.5 Tesla) was significantly higher with DCE–MRI and 3D MRSI than with T2-weighted imaging[14,15]. Using a 3.0-Tesla system, Kim *et al*[16] found that detection of prostate cancer in the peripheral zone was better with DCE-MRI than with T2-weighted imaging. Sensitivity, specificity, and accuracy were 55%, 88% and 70%, respectively, with T2-weighted MRI as compared to 73%, 77%, and 75%, respectively, with dynamic contrast-enhanced imaging. In another study phased-array coils were used for signal homogeneity to image patients on a 1.5 T system before biopsy; based on early and intense enhancement areas on T1-weighted DCE images, sensitivity, specificity, and positive and negative predictive values were 90%, 88%, 77% and 95%, respectively for the detection of foci greater than 0.5 cc *vs* 77%, 91%, 86% and 85% for the detection of foci greater than 0.2 cc[17]. Ocak *et al*[18] found the forward volume transfer constant (K^{trans}), the reverse reflux rate constant between extracellular space and plasma (k_{ep}), and the area under the gadolinium curve (AUGC) to be significantly higher in cancer than in the normal PZ. Engelbrecht *et al*[19] identified relative peak enhancement in the PZ and washout rate in the central gland as DCE-MRI parameters useful for prostate cancer detection and localization, but they did not find strong correlations between dynamic parameters in prostate

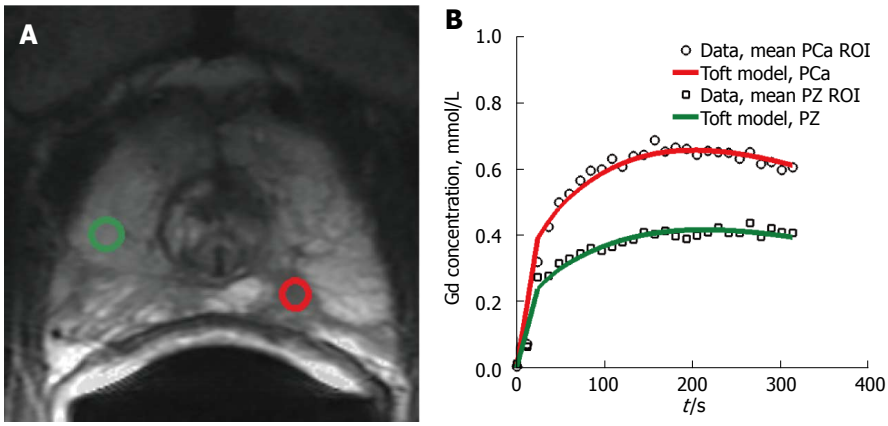

Figure 3 Example of enhancement kinetics pattern from two regions-of-interest. A: Transverse T2-weighted image. The green regions-of-interest (ROIs) corresponds to a benign PZ region. The red ROI corresponds to region with prostate cancer; B: Contrast curves of the two ROIs shown in A. The curves are characteristic of the types of time-intensity curves obtained with dynamic contrast-enhanced MRI. The green ROI shows moderately slow and slight enhancement wash-in pattern. This is characteristic for many benign, enhancing tissues, such as normal prostate tissue. The red ROI shows a rapid rise in signal intensity with subsequent wash-out as is typical in tumors.

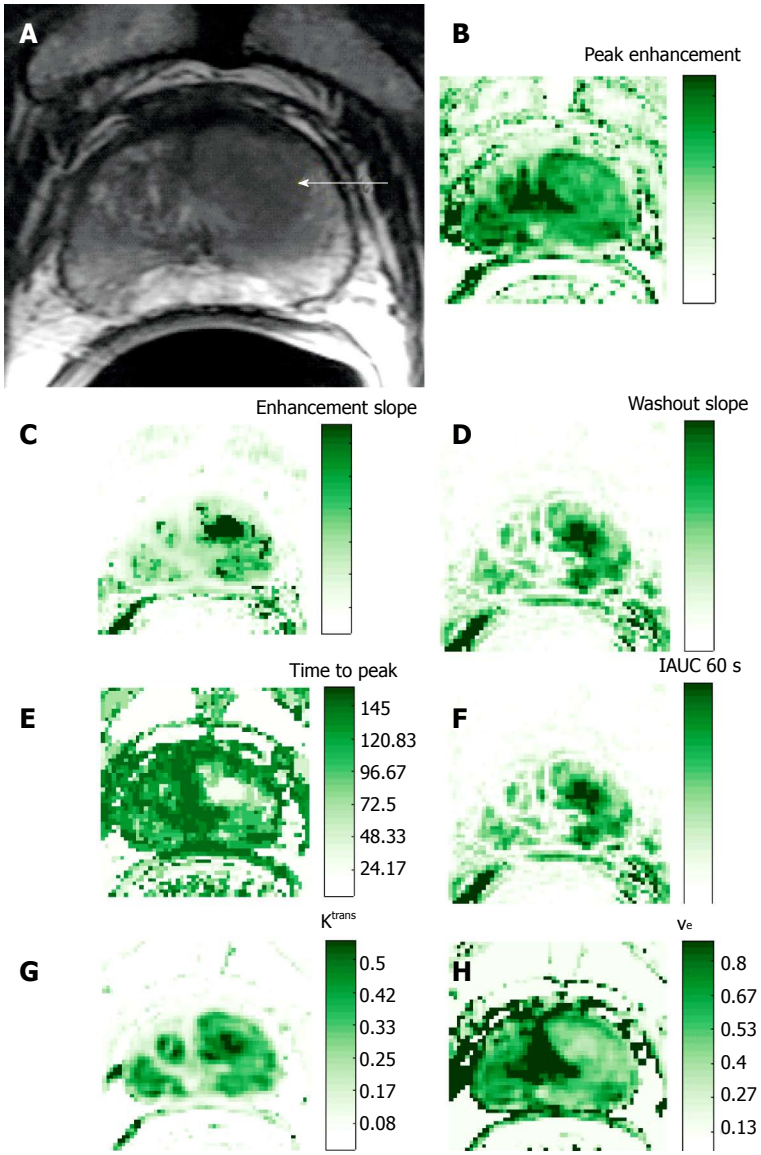

Figure 4 Representative 3T data in 63-year-old patient with prostate cancer (presurgical prostate-specific antigen level, 3.4 ng/mL). A: Transverse T2-weighted image. Pharmacokinetic parameter maps based on the semi-quantitative method and the Toft's kinetic model. Parametric maps for the semi-quantitative parameters, including; B: Peak-enhancement; C: Enhancement slope; D: Wash-out slope; E: Time-to-peak; and F: Intensity curve or contrast medium concentration at 60 s. Using the Toft's kinetic model, the pharmacokinetic parameter maps for G K^{trans} and H v_e are shown.

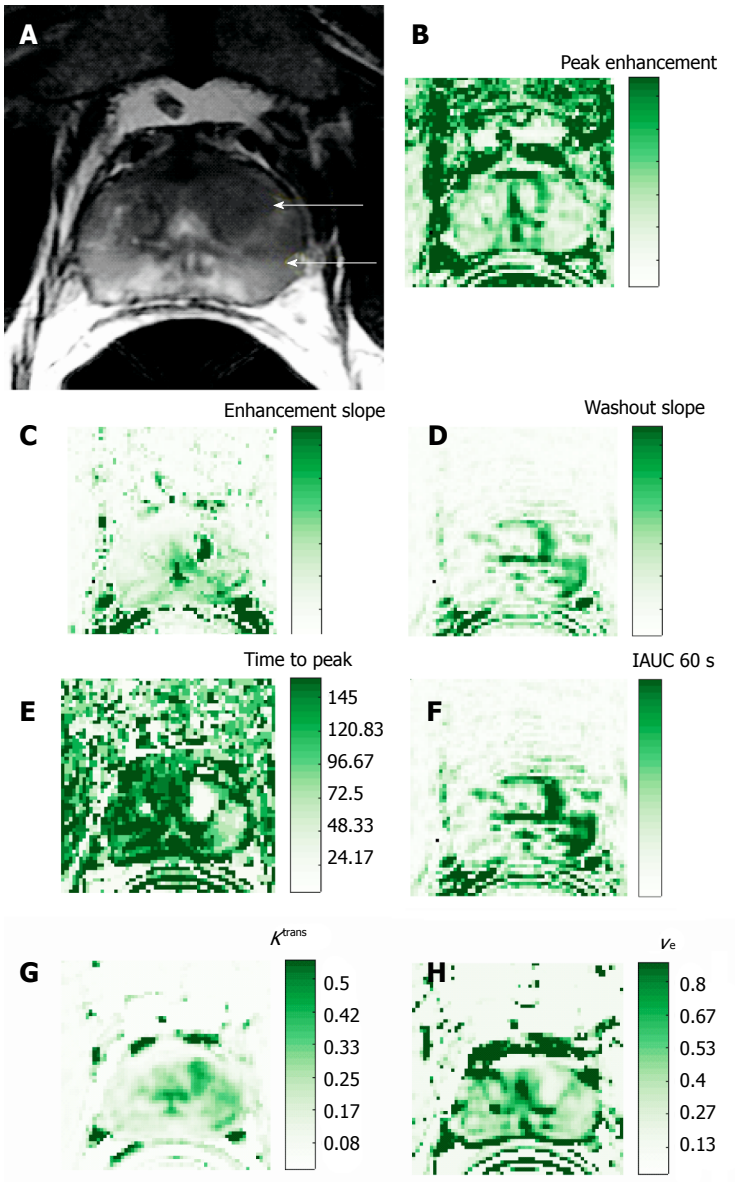

Figure 5 Representative 3T data in a 54-year-old prostate cancer patient [presurgical prostate-specific antigen level, 4.7 ng/mL; biopsy Gleason score, 7 (3 + 4)]. Pharmacokinetic parameter maps based on the semi-quantitative method and the Toft's kinetic model. Parametric maps for the semi-quantitative parameters, including B: Peak-enhancement; C: Enhancement slope; D: Wash-out slope; E: Time-to-peak; and F: Intensity curve or contrast medium concentration at 60 s. Using the Toft's kinetic model, the pharmacokinetic parameter maps for G K^{trans} and H v_e are shown.

cancer regions and tumor stage, Gleason score, patient age, tumor volume, or prostate-specific antigen. Alonzi *et al*[20] provided a table summarizing the early literature on prostate tumor localization.

With regard to staging of prostate cancer with DCE-MRI, one study compared the performance of an experienced reader to that of a less experienced reader[21]. The investigators found that for the experienced reader, the sensitivity, specificity, and accuracy of staging with dynamic contrast-enhanced MR imaging were 69%, 97%, and 87%, respectively, and were not significantly different from the corresponding values obtained with T2-weighted imaging alone. However, for the less experienced reader, the use of DCE-MRI parametric maps resulted in a significant improvement in the area under the receiver operating characteristic curve as compared to T2-weighted imaging alone. Bloch *et al*[22] presented findings from 1.5-Tesla high-spatial-resolution T2-weighted imaging and DCE-MR imaging in 32 patients. When the T2-weighted imaging and DCE-MR imaging data sets were combined, the mean sensitivity, specificity, *P* value, and negative predictive values for the assessment of extracapsular extension (ECE) were 86%, 95%, 90%, and 93%, respectively; the determination of ECE was significantly better when the data sets were combined than when T2-weighted imaging was used alone.

ROLE OF DCE-MRI IN THE PI-RADS (PROSTATE IMAGING REPORTING AND DATA SYSTEM) CLASSIFICATION

The European Society of Urogenital Radiology (ESUR) has provided a set of guidelines for MR imaging of the

prostate[23]. These guidelines provide recommendations for minimum standards of MR protocols as well outlining a structured reporting scheme, referred to as PI-RADS which are based on the BI-RADS classification for breast imaging. The reporting provides scores ranging from 1 to 5. The PI-RADS classification of DCE-MRI uses the time-resolved signal intensity curve to provide a qualitative analysis of the shape of the signal intensity curve. A score of 1 is assigned when the signal intensity curve increases gradually (Type Ⅰ curve). Score of 2 is assigned when there is progressive signal intensity stabilization followed by a slight and late decrease in signal intensity (Type Ⅱ curve). Score of 3 is assigned if the signal intensity curve demonstrates rapid washout after reaching peak enhancement (Type Ⅲ curve). Focal lesions which enhance according to Type Ⅱ or Ⅲ curves are assigned an additional point. Asymmetric lesions or unusually located lesions which enhance according to Type Ⅱ or Ⅲ curves receive an additional point[24].

Assessment of prostate cancer aggressiveness

The Gleason score, determined by histopathology, characterizes prostate cancer aggressiveness based on the microscopic appearance of the cancer tissue[25]. Together with other parameters, the Gleason score is used for prostate cancer staging, assessment of the patient's prognosis and treatment selection. Most commonly, the Gleason score is determined by biopsy, which is performed when an elevated serum prostate-specific antigen (PSA) level and/or an abnormal digital rectal examination (DRE) suggest that the patient may have prostate cancer. The biopsy Gleason score and the amount of cancer in each biopsy core are both important predictors of prostate cancer aggressiveness and rate of progression[26,27]. However, biopsy underestimates the Gleason score relative to the prostatectomy Gleason score in as many as 50% of cases[28]. Moreover, sextant biopsy samples mostly the posterior peripheral zone of the prostate, thereby potentially missing tumors in anterior portions of the gland.

A review of prior studies to identify associations between MRI perfusion parameters and Gleason score suggests no such associations have been consistently found[29-33]. An earlier study by Padhani *et al*[29] found only a weak correlation between MRI tumor stage and tumor vascular permeability. However, no correlation was observed between enhancement patterns (*i.e.*, both quantitive and semi-quantitive parameters) and Gleason score or PSA levels. Another study used an enhanced inversion-prepared dual-contrast gradient-echo sequence at 1.5 Tesla to perform DCE-MRI combined with dynamic susceptibility contrast (DSC) MR imaging, which allows simultaneous calculation of the parameters blood volume, blood flow, and interstitial volume. Subsequently, the parameters were correlated with histologic mean vessel density (MVD), mean vessel area (MVA), and mean interstitial area (MIA), and it was found that the measured quantities of blood volume and interstitial volume did not reliably correlate with the histologic parameters[30]. Chen *et al*[31] performed both semi-quantitative and quantitaive analysis of DCE-MRI and correlated the parameters with Gleason score; they found that only the washout gradient correlated significantly with Gleason score. Another study using quantitaive analysis of DCE-MRI was also unable to identify any significant correlations with Gleason score or vascular endothelial growth factor (VEGF) expression, although k_{ep} was found to correlate moderately with microvessel density[32]. Recently, a study at 3 Tesla found that both semi-quantitative and quantitative parameters (mean and 75th percentile values of wash-in, mean wash-out, and 75th percentile of K^{trans}), differed significantly between low-grade (Gleason grades 2 and 3 present) and high-grade prostate cancer (primary Gleason grade of 4 and/or any 5 component) in the peripheral zone[33]. Two factors which were identified as being important in acquisition of data for optimal modeling were: (1) the use of high temporal resolution imaging (temporal resolution = 3 s), which allowed the investigators to more accurately probe the early phase of enhancement; and (2) the use of patient-specific AIF rather than population-based AIF.

ASSESSMENT OF TREATMENT RESPONSE

Androgen deprivation therapy

VEGF also called vascular permeability factor, is a stimulus of tumor neo-angiogenesis[34]. It has been shown that androgens induce the simulation of vascular endothelial growth factor production in human prostate cancer[35]. A study of 56 patients measured the effects of androgen deprivation therapy (ADT) on prostatic morphology and vascular permeability[36] and found a significant reduction in tumor permeability surface area product in the peripheral zone, central gland and tumor, as well as changes in washout patterns[36]. The authors also reported significant reductions in K^{trans} in the peripheral zone and central gland as well as a weak correlation between tumor K^{trans} and tumor volume change.

Another study examined the effect of ADT on prostate tumor blood flow by comparing quantitative parametric maps of the prostate for blood flow, blood volume, and blood oxygenation [intrinsic relaxivity (R_2*)], measured using a DSC-MRI acquisition and analysis, and K^{trans} and v_e, measured using a DCE-MRI acquisition and analysis; values acquired before ADT was administered were compared to those acquired after 1 mo and 3 mo of therapy[37]. The study found significant decreases in tumor blood volume and flow in the first month after treatment, and significant increases in R_2* of the prostate tumor by three months; the study also found significant reductions in tumor K^{trans} from baseline at both 1 and 3 mo. Another study looking at monitoring response with both DCE and DWI found that DCE-MRI parameters (K^{trans}, v_e, v_p, IAUGC-90) measured in tumor after 3 mo of therapy were significantly reduced as compared to those

measured before treatment, whereas normal-appearing peripheral zone tissue showed no significant change[38].

External-beam radiation therapy

When local recurrence is suspected after radiation treatment, MRI may be used to identify a target for biopsy and estimate the location and extent of the tumor. In an early study by Rouvière *et al*[39] assessing the value of DCE-MRI in patients with suspected recurrent prostate cancer after external beam radiotherapy (EBRT), readers interpreted contrast-enhanced images during the early phases, when prostatic tissue showed some degree of enhancement (the images were referred to as arterial phase images). They found that as compared to T2-weighted imaging, contrast-enhanced MRI localized recurrent cancer after EBRT more accurately and with less inter-observer variability. A later study found that in the localization of recurrent prostate cancer by sextant in patients with suspected relapse after EBRT, the sensitivity, positive predictive value and negative predictive value of DCE-MRI were significantly higher than those of T2-weighted imaging[40]. Although the investigators found that DCE-MRI had excellent sensitivity, negative predictive value (both of 100%), and good accuracy (82%) for the detection of prostate cancer recurrence after EBRT, the positive predictive value was not very high (46%), even though it was higher than that of T2-weighted imaging. Multi-parametric approaches have also been investigated[41,42]. One recent study found multi-parametric methods to be superior to T2-weighted imaging in the detection of recurrent prostate cancer after image-guided radiation therapy; however, there was no additional benefit when DCE-MRI was added to combined T2-weighed imaging and diffusion-weighted MRI (DW-MRI)[42].

High-dose-rate brachytherapy

A recent article retrospectively evaluated the ability of multiphase (specifically, 5-phase) dynamic contrast-enhanced MRI obtained every 30 s (as well as DW-MRI) to detect local recurrence after high-dose-rate brachytherapy[43]. Whereas the sensitivity, specificity, and accuracy of T2-weighted imaging were 27%, 99%, and 87%, respectively, those of DCE-MRI were 50%, 98%, and 90%, respectively. The authors found that a multi-parametric approach combining T2-weighted MRI, DW-MRI and DCE-MRI achieved the highest sensitivity (77%) with a slight reduction in specificity (92%) as compared to DW-MRI.

High-intensity focused ultrasound

For the treatment of patients with localized prostate cancer, a nonsurgical, noninvasive treatment referred to as transrectal high-intensity focused ultrasound (HIFU) can be considered[44,45]. DCE-MRI (combined with T2-weighted imaging) can have a role in detecting local cancer recurrences after HIFU. It can assist in distinguishing residual or recurrent cancers within 2-5 d after HIFU treatment[46] which are typically hypervascular from post-HIFU fibrosis which are often homogeneous and hypovascular[47] and can guide post-HIFU biopsy towards areas of recurrent cancer. One study found that although Gadolinium-enhanced MRI can accurately determine the extend of tissue damage following HIFU, it cannot predict histological results[46].

Surgery

A study by Casciani *et al*[48] to determine the ability of endorectal MRI (T1- and T2-weighted imaging) combined with DCE-MRI to detect local recurrence after radical prostatectomy found that all recurrences showed signal enhancement after gadolinium administration. In most cases of recurrence (22/24), tumors display rapid and early signal enhancement. The study found a significant improvement in the detection of recurrence with combined MRI and DCE-MRI as compared to MRI alone. Similarly, Sciarra *et al*[49] found that the use of DCE-MRI alone or in combination with spectroscopic imaging was accurate for identifying local prostate cancer recurrence in patients with biochemical progression after radical prostatectomy.

CHALLENGES AND FUTURE DIRECTIONS

Limitations in DCE-MRI specific to prostate cancer include motion artifact, specifically from rectal and colonic peristalsis. Further, hyperintense findings on MRI may correlate not only with abnormal tumor tissue but any changes in vascularity including BPH nodules, post-biopsy changes, and prostatitis. At present, an additional limitation of DCE-MRI of the prostate, which also applies to the imaging of all other organ systems, is the lack of standardization of sequences and analysis parameters[5]. With the availability of a wide range of imaging sequences on most MR units, a defining objective of many studies today is to identify the role of DCE-MRI as part of a multi-parametric examination[50].

CONCLUSION

We have reviewed DCE-MRI acquisition and data analysis methods for the detection and monitoring of cancer in the prostate. Potential clinical applications of DCE-MRI for prostate cancer include detection, localization and staging, assessment of tumor aggressiveness, and assessment of treatment response. Limitations include lack of standardized acquisition and analysis methods which can results in variability in the results. We expect that with the standardization of these methods will encourage more wide spread use of DCE-MRI in prostate cancer imaging.

REFERENCES

1 **Padhani AR**, Husband JE. Dynamic contrast-enhanced MRI studies in oncology with an emphasis on quantification, validation and human studies. *Clin Radiol* 2001; **56**: 607-620 [PMID: 11467863 DOI: 10.1053/crad.2001.0762]

2 **Knopp MV**, Giesel FL, Marcos H, von Tengg-Kobligk H, Choyke P. Dynamic contrast-enhanced magnetic resonance imaging in oncology.

Top Magn Reson Imaging 2001; **12**: 301-308 [PMID: 11687716]
3 **Tofts PS**, Brix G, Buckley DL, Evelhoch JL, Henderson E, Knopp MV, Larsson HB, Lee TY, Mayr NA, Parker GJ, Port RE, Taylor J, Weisskoff RM. Estimating kinetic parameters from dynamic contrast-enhanced T(1)-weighted MRI of a diffusable tracer: standardized quantities and symbols. *J Magn Reson Imaging* 1999; **10**: 223-232 [PMID: 10508281]
4 **Sourbron SP**, Buckley DL. Classic models for dynamic contrast-enhanced MRI. *NMR Biomed* 2013; **26**: 1004-1027 [PMID: 23674304 DOI: 10.1002/nbm.2940]
5 **Verma S**, Turkbey B, Muradyan N, Rajesh A, Cornud F, Haider MA, Choyke PL, Harisinghani M. Overview of dynamic contrast-enhanced MRI in prostate cancer diagnosis and management. *AJR Am J Roentgenol* 2012; **198**: 1277-1288 [PMID: 22623539 DOI: 10.2214/AJR.12.8510]
6 **Ferl GZ**, Port RE. Quantification of antiangiogenic and antivascular drug activity by kinetic analysis of DCE-MRI data. *Clin Pharmacol Ther* 2012; **92**: 118-124 [PMID: 22588603 DOI: 10.1038/clpt.2012.63]
7 **Donahue KM**, Burstein D, Manning WJ, Gray ML. Studies of Gd-DTPA relaxivity and proton exchange rates in tissue. *Magn Reson Med* 1994; **32**: 66-76 [PMID: 8084239]
8 **Tofts PS**. Modeling tracer kinetics in dynamic Gd-DTPA MR imaging. *J Magn Reson Imaging* 1997; **7**: 91-101 [PMID: 9039598]
9 **Brix G**, Bahner ML, Hoffmann U, Horvath A, Schreiber W. Regional blood flow, capillary permeability, and compartmental volumes: measurement with dynamic CT--initial experience. *Radiology* 1999; **210**: 269-276 [PMID: 9885619 DOI: 10.1148/radiology.210.1.r99ja46269]
10 **Weinmann HJ**, Laniado M, Mützel W. Pharmacokinetics of GdDTPA/dimeglumine after intravenous injection into healthy volunteers. *Physiol Chem Phys Med NMR* 1984; **16**: 167-172 [PMID: 6505043]
11 **Meng R**, Chang SD, Jones EC, Goldenberg SL, Kozlowski P. Comparison between population average and experimentally measured arterial input function in predicting biopsy results in prostate cancer. *Acad Radiol* 2010; **17**: 520-525 [PMID: 20074982 DOI: 10.1016/j.acra.2009.11.006]
12 **Fedorov A**, Fluckiger J, Ayers GD, Li X, Gupta SN, Tempany C, Mulkern R, Yankeelov TE, Fennessy FM. A comparison of two methods for estimating DCE-MRI parameters via individual and cohort based AIFs in prostate cancer: a step towards practical implementation. *Magn Reson Imaging* 2014; **32**: 321-329 [PMID: 24560287 DOI: 10.1016/j.mri.2014.01.004]
13 **Fennessy FM**, Fedorov A, Gupta SN, Schmidt EJ, Tempany CM, Mulkern RV. Practical considerations in T1 mapping of prostate for dynamic contrast enhancement pharmacokinetic analyses. *Magn Reson Imaging* 2012; **30**: 1224-1233 [PMID: 22898681 DOI: 10.1016/j.mri.2012.06.011]
14 **Fütterer JJ**, Heijmink SW, Scheenen TW, Veltman J, Huisman HJ, Vos P, Hulsbergen-Van de Kaa CA, Witjes JA, Krabbe PF, Heerschap A, Barentsz JO. Prostate cancer localization with dynamic contrast-enhanced MR imaging and proton MR spectroscopic imaging. *Radiology* 2006; **241**: 449-458 [PMID: 16966484 DOI: 10.1148/radiol.2412051866]
15 **Fütterer JJ**, Heijmink SW, Scheenen TW, Jager GJ, Hulsbergen-Van de Kaa CA, Witjes JA, Barentsz JO. Prostate cancer: local staging at 3-T endorectal MR imaging--early experience. *Radiology* 2006; **238**: 184-191 [PMID: 16304091 DOI: 10.1148/radiol.2381041832]
16 **Kim CK**, Park BK, Kim B. Localization of prostate cancer using 3T MRI: comparison of T2-weighted and dynamic contrast-enhanced imaging. *J Comput Assist Tomogr* 2006; **30**: 7-11 [PMID: 16365565]
17 **Villers A**, Puech P, Mouton D, Leroy X, Ballereau C, Lemaitre L. Dynamic contrast enhanced, pelvic phased array magnetic resonance imaging of localized prostate cancer for predicting tumor volume: correlation with radical prostatectomy findings. *J Urol* 2006; **176**: 2432-2437 [PMID: 17085122 DOI: 10.1016/j.juro.2006.08.007]
18 **Ocak I**, Bernardo M, Metzger G, Barrett T, Pinto P, Albert PS, Choyke PL. Dynamic contrast-enhanced MRI of prostate cancer at 3 T: a study of pharmacokinetic parameters. *AJR Am J Roentgenol* 2007; **189**: 849 [PMID: 17885055 DOI: 10.2214/AJR.06.1329]
19 **Engelbrecht MR**, Huisman HJ, Laheij RJ, Jager GJ, van Leenders GJ, Hulsbergen-Van De Kaa CA, de la Rosette JJ, Blickman JG, Barentsz JO. Discrimination of prostate cancer from normal peripheral zone and central gland tissue by using dynamic contrast-enhanced MR imaging. *Radiology* 2003; **229**: 248-254 [PMID: 12944607 DOI: 10.1148/radiol.2291020200]
20 **Alonzi R**, Padhani AR, Allen C. Dynamic contrast enhanced MRI in prostate cancer. *Eur J Radiol* 2007; **63**: 335-350 [PMID: 17689907 DOI: 10.1016/j.ejrad.2007.06.028]
21 **Fütterer JJ**, Engelbrecht MR, Huisman HJ, Jager GJ, Hulsbergen-van De Kaa CA, Witjes JA, Barentsz JO. Staging prostate cancer with dynamic contrast-enhanced endorectal MR imaging prior to radical prostatectomy: experienced versus less experienced readers. *Radiology* 2005; **237**: 541-549 [PMID: 16244263 DOI: 10.1148/radiol.2372041724]
22 **Bloch BN**, Furman-Haran E, Helbich TH, Lenkinski RE, Degani H, Kratzik C, Susani M, Haitel A, Jaromi S, Ngo L, Rofsky NM. Prostate cancer: accurate determination of extracapsular extension with high-spatial-resolution dynamic contrast-enhanced and T2-weighted MR imaging--initial results. *Radiology* 2007; **245**: 176-185 [PMID: 17717328 DOI: 10.1148/radiol.2451061502]
23 **Barentsz JO**, Richenberg J, Clements R, Choyke P, Verma S, Villeirs G, Rouviere O, Logager V, Fütterer JJ; European Society of Urogenital Radiology. ESUR prostate MR guidelines 2012. *Eur Radiol* 2012; **22**: 746-757 [PMID: 22322308 DOI: 10.1007/s00330-011-2377-y]
24 **Röthke M**, Blondin D, Schlemmer HP, Franiel T. [PI-RADS classification: structured reporting for MRI of the prostate]. *Rofo* 2013; **185**: 253-261 [PMID: 23404430]
25 **Gleason DF**, Mellinger GT. Prediction of prognosis for prostatic adenocarcinoma by combined histological grading and clinical staging. *J Urol* 1974; **111**: 58-64 [PMID: 4813554]
26 **Epstein JI**, Allsbrook WC Jr, Amin MB, Egevad LL. Update on the Gleason grading system for prostate cancer: results of an international consensus conference of urologic pathologists. *Adv Anat Pathol* 2006; **13**: 57-59 [PMID: 16462155 DOI: 10.1097/01.pap.0000202017.78917.18]
27 **Epstein JI**. What's new in prostate cancer disease assessment in 2006? *Curr Opin Urol* 2006; **16**: 146-151 [PMID: 16679850 DOI: 10.1097/01.mou.0000193389.31727.9b]
28 **Bak JB**, Landas SK, Haas GP. Characterization of prostate cancer missed by sextant biopsy. *Clin Prostate Cancer* 2003; **2**: 115-118 [PMID: 15040873]
29 **Padhani AR**, Gapinski CJ, Macvicar DA, Parker GJ, Suckling J, Revell PB, Leach MO, Dearnaley DP, Husband JE. Dynamic contrast enhanced MRI of prostate cancer: correlation with morphology and tumour stage, histological grade and PSA. *Clin Radiol* 2000; **55**: 99-109 [PMID: 10657154 DOI: 10.1053/crad.1999.0327]
30 **Franiel T**, Lüdemann L, Rudolph B, Rehbein H, Stephan C, Taupitz M, Beyersdorff D. Prostate MR imaging: tissue characterization with pharmacokinetic volume and blood flow parameters and correlation with histologic parameters. *Radiology* 2009; **252**: 101-108 [PMID: 19561252 DOI: 10.1148/radiol.2521081400]
31 **Chen M**, Dang HD, Wang JY, Zhou C, Li SY, Wang WC, Zhao WF, Yang ZH, Zhong CY, Li GZ. Prostate cancer detection: comparison of T2-weighted imaging, diffusion-weighted imaging, proton magnetic resonance spectroscopic imaging, and the three techniques combined. *Acta Radiol* 2008; **49**: 602-610 [PMID: 18568549 DOI: 10.1080/02841850802004983]
32 **Oto A**, Kayhan A, Jiang Y, Tretiakova M, Yang C, Antic T, Dahi F, Shalhav AL, Karczmar G, Stadler WM. Prostate cancer: differentiation of central gland cancer from benign prostatic hyperplasia by using diffusion-weighted and dynamic contrast-enhanced MR imaging. *Radiology* 2010; **257**: 715-723 [PMID: 20843992 DOI: 10.1148/radiol.10100021]
33 **Vos EK**, Litjens GJ, Kobus T, Hambrock T, Hulsbergen-van de Kaa CA, Barentsz JO, Huisman HJ, Scheenen TW. Assessment of prostate cancer aggressiveness using dynamic contrast-enhanced magnetic resonance imaging at 3 T. *Eur Urol* 2013; **64**: 448-455 [PMID: 23751135 DOI: 10.1016/j.eururo.2013.05.045]

34 **Dvorak HF**, Brown LF, Detmar M, Dvorak AM. Vascular permeability factor/vascular endothelial growth factor, microvascular hyperpermeability, and angiogenesis. *Am J Pathol* 1995; **146**: 1029-1039 [PMID: 7538264]

35 **Häggström S**, Lissbrant IF, Bergh A, Damber JE. Testosterone induces vascular endothelial growth factor synthesis in the ventral prostate in castrated rats. *J Urol* 1999; **161**: 1620-1625 [PMID: 10210429]

36 **Padhani AR**, MacVicar AD, Gapinski CJ, Dearnaley DP, Parker GJ, Suckling J, Leach MO, Husband JE. Effects of androgen deprivation on prostatic morphology and vascular permeability evaluated with mr imaging. *Radiology* 2001; **218**: 365-374 [PMID: 11161148 DOI: 10.1148/radiology.218.2.r01ja04365]

37 **Alonzi R**, Padhani AR, Taylor NJ, Collins DJ, D'Arcy JA, Stirling JJ, Saunders MI, Hoskin PJ. Antivascular effects of neoadjuvant androgen deprivation for prostate cancer: an in vivo human study using susceptibility and relaxivity dynamic MRI. *Int J Radiat Oncol Biol Phys* 2011; **80**: 721-727 [PMID: 20630668 DOI: 10.1016/j.ijrobp.2010.02.060]

38 **Barrett T**, Gill AB, Kataoka MY, Priest AN, Joubert I, McLean MA, Graves MJ, Stearn S, Lomas DJ, Griffiths JR, Neal D, Gnanapragasam VJ, Sala E. DCE and DW MRI in monitoring response to androgen deprivation therapy in patients with prostate cancer: a feasibility study. *Magn Reson Med* 2012; **67**: 778-785 [PMID: 22135228]

39 **Rouvière O**, Valette O, Grivolat S, Colin-Pangaud C, Bouvier R, Chapelon JY, Gelet A, Lyonnet D. Recurrent prostate cancer after external beam radiotherapy: value of contrast-enhanced dynamic MRI in localizing intraprostatic tumor--correlation with biopsy findings. *Urology* 2004; **63**: 922-927 [PMID: 15134982 DOI: 10.1016/j.urology.2003.12.017]

40 **Haider MA**, Chung P, Sweet J, Toi A, Jhaveri K, Ménard C, Warde P, Trachtenberg J, Lockwood G, Milosevic M. Dynamic contrast-enhanced magnetic resonance imaging for localization of recurrent prostate cancer after external beam radiotherapy. *Int J Radiat Oncol Biol Phys* 2008; **70**: 425-430 [PMID: 17881141 DOI: 10.1016/j.ijrobp.2007.06.029]

41 **Akin O**, Gultekin DH, Vargas HA, Zheng J, Moskowitz C, Pei X, Sperling D, Schwartz LH, Hricak H, Zelefsky MJ. Incremental value of diffusion weighted and dynamic contrast enhanced MRI in the detection of locally recurrent prostate cancer after radiation treatment: preliminary results. *Eur Radiol* 2011; **21**: 1970-1978 [PMID: 21533634]

42 **Donati OF**, Jung SI, Vargas HA, Gultekin DH, Zheng J, Moskowitz CS, Hricak H, Zelefsky MJ, Akin O. Multiparametric prostate MR imaging with T2-weighted, diffusion-weighted, and dynamic contrast-enhanced sequences: are all pulse sequences necessary to detect locally recurrent prostate cancer after radiation therapy? *Radiology* 2013; **268**: 440-450 [PMID: 23481164 DOI: 10.1148/radiol.13122149]

43 **Tamada T**, Sone T, Higashi H, Jo Y, Yamamoto A, Kanki A, Ito K. Prostate cancer detection in patients with total serum prostate-specific antigen levels of 4-10 ng/mL: diagnostic efficacy of diffusion-weighted imaging, dynamic contrast-enhanced MRI, and T2-weighted imaging. *AJR Am J Roentgenol* 2011; **197**: 664-670 [PMID: 21862809 DOI: 10.2214/AJR.10.5923]

44 **Uchida T**, Ohkusa H, Yamashita H, Shoji S, Nagata Y, Hyodo T, Satoh T. Five years experience of transrectal high-intensity focused ultrasound using the Sonablate device in the treatment of localized prostate cancer. *Int J Urol* 2006; **13**: 228-233 [PMID: 16643614]

45 **Poissonnier L**, Chapelon JY, Rouvière O, Curiel L, Bouvier R, Martin X, Dubernard JM, Gelet A. Control of prostate cancer by transrectal HIFU in 227 patients. *Eur Urol* 2007; **51**: 381-387 [PMID: 16857310 DOI: 10.1016/j.eururo.2006.04.012]

46 **Rouvière O**, Lyonnet D, Raudrant A, Colin-Pangaud C, Chapelon JY, Bouvier R, Dubernard JM, Gelet A. MRI appearance of prostate following transrectal HIFU ablation of localized cancer. *Eur Urol* 2001; **40**: 265-274 [PMID: 11684842]

47 **Rouvière O**, Girouin N, Glas L, Ben Cheikh A, Gelet A, Mège-Lechevallier F, Rabilloud M, Chapelon JY, Lyonnet D. Prostate cancer transrectal HIFU ablation: detection of local recurrences using T2-weighted and dynamic contrast-enhanced MRI. *Eur Radiol* 2010; **20**: 48-55 [PMID: 19690866 DOI: 10.1007/s00330-009-1520-5]

48 **Casciani E**, Polettini E, Carmenini E, Floriani I, Masselli G, Bertini L, Gualdi GF. Endorectal and dynamic contrast-enhanced MRI for detection of local recurrence after radical prostatectomy. *AJR Am J Roentgenol* 2008; **190**: 1187-1192 [PMID: 18430830 DOI: 10.2214/AJR.07.3032]

49 **Sciarra A**, Panebianco V, Salciccia S, Osimani M, Lisi D, Ciccariello M, Passariello R, Di Silverio F, Gentile V. Role of dynamic contrast-enhanced magnetic resonance (MR) imaging and proton MR spectroscopic imaging in the detection of local recurrence after radical prostatectomy for prostate cancer. *Eur Urol* 2008; **54**: 589-600 [PMID: 18226441 DOI: 10.1016/j.eururo.2007.12.034]

50 **Puech P**, Sufana-Iancu A, Renard B, Lemaitre L. Prostate MRI: can we do without DCE sequences in 2013? *Diagn Interv Imaging* 2013; **94**: 1299-1311 [PMID: 24211261 DOI: 10.1016/j.diii.2013.09.010]

P- Reviewer: Arcangeli S, Shoji S **S- Editor**: Cui LJ **L- Editor**: A **E- Editor**: Lu YJ

Published by **Baishideng Publishing Group Inc**
7901 Stoneridge Drive, Suite 501, Pleasanton, CA 94588, USA
Telephone: +1-925-223-8242
Fax: +1-925-223-8243
E-mail: bpgoffice@wjgnet.com
Help Desk: http://www.f6publishing.com/helpdesk
http://www.wjgnet.com